

Impacts of the 2014-2015 warm-water anomalies on nutrients, chlorophyll-a and hydrographic conditions in the coastal zone of northern Baja California

Francisco Delgadillo-Hinojosa¹, Armando Félix-Bermúdez¹, Eunise Vanessa Torres-Delgado², Reginaldo Durazo³, Victor Camacho-Ibar¹, Adán Mejía-Trejo², Mary Carmen Ruiz-de la Torre³, and Lorena Linacre⁴

¹Universidad Autónoma de Baja California

²Universidad Autónoma de Baja California.

³Universidad Autonoma de Baja California

⁴CICESE

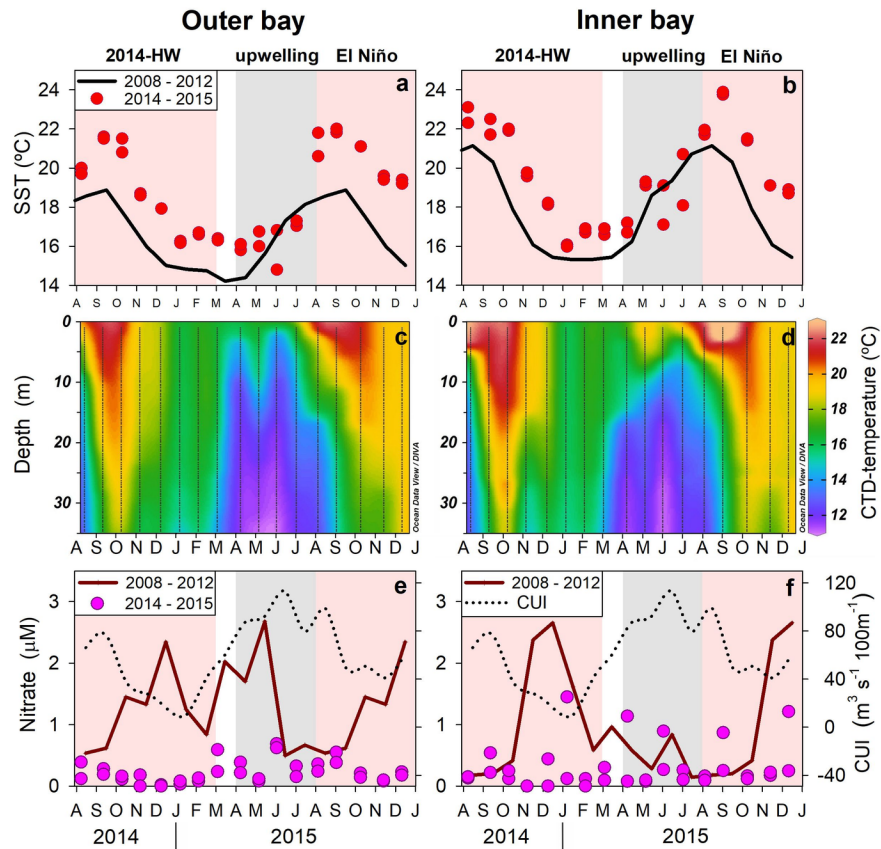
November 21, 2022

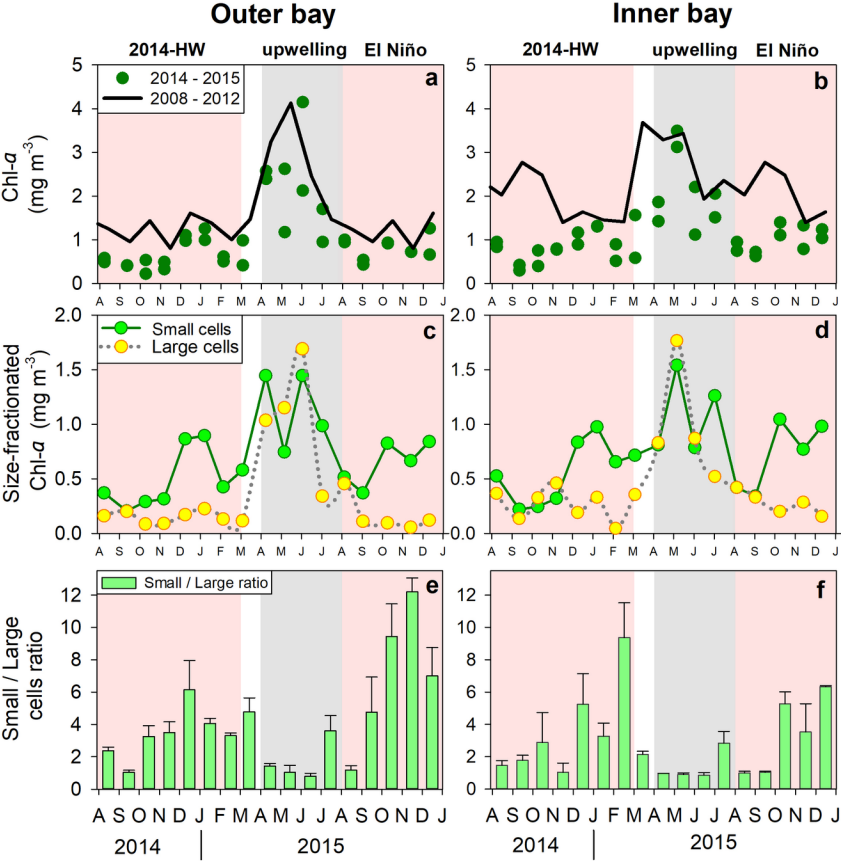
Abstract

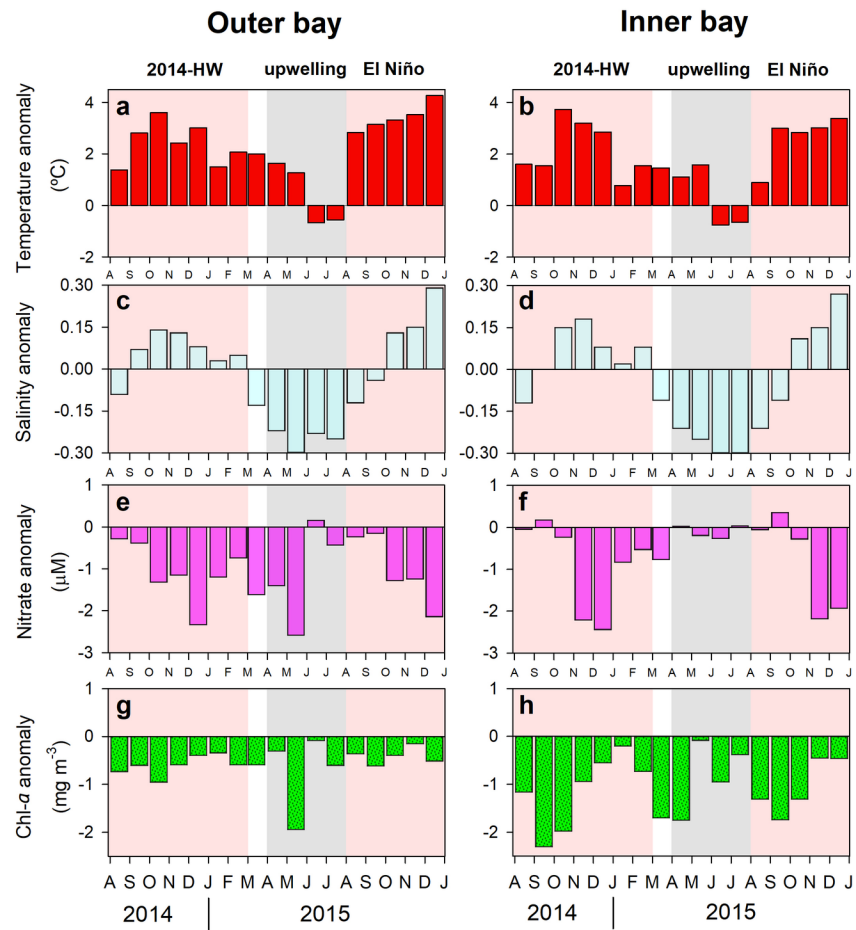
We report the seasonal variability of temperature, nutrients, and total and size fractionated chlorophyll- in nearshore waters off northern Baja California (nBC), under conditions of the marine heatwave and El Niño that occurred in the northeastern Pacific during 2014-2015. Compared with 2008-2012, our study period was characterized by warmer waters, nitrate-impooverished and with very low chlorophyll- concentration, which was closely associated with strong stratification and reduced upwelling conditions off nBC. Temperature anomalies were $>3.0^{\circ}\text{C}$ by the end of 2014 when the marine heatwave prevailed, decreased during the spring-early summer upwelling season of 2015, and returned to $>3.5^{\circ}\text{C}$ by the end of 2015 when El Nino appeared along the coast of nBC. As in 2008-2012 and closely coupled with upwelling, a clear seasonal cycle of total chlorophyll- was recorded under these abnormally warm conditions. However, total chlorophyll- and nitrate concentrations were significantly reduced (25-68% and 33-90%, respectively), with negative anomalies throughout the study period. Moreover, the seasonal evolution of the size-fractionated chlorophyll- concentration showed that smaller cells ($<5\text{ }\mu\text{m}$) systematically contributed with the largest fraction ($>60\%$) of the total chlorophyll-. Our findings indicate that the sequential occurrence of the marine heatwave in 2014 and El Nino in 2015, had a significant and sustained impact limiting the nitrate supply and reducing the total chlorophyll- in nearshore waters off nBC. In conclusion, our data reveal that a shift towards an oligotrophic state occurred in nearshore surface waters off northern Baja California during the warm period of 2014-2015.

Hosted file

table_i.docx available at <https://authorea.com/users/530941/articles/597503-impacts-of-the-2014-2015-warm-water-anomalies-on-nutrients-chlorophyll-a-and-hydrographic-conditions-in-the-coastal-zone-of-northern-baja-california>







Impacts of the 2014-2015 warm-water anomalies on nutrients, chlorophyll-*a* and hydrographic conditions in the coastal zone of northern Baja California

Delgadillo-Hinojosa, F.^{1*}, Félix-Bermúdez, A.¹, Torres-Delgado, E.V.¹, Durazo, R.², Camacho-Ibar, V.¹, Mejía, A.¹, Ruiz, M.C.², Linacre, L.³

¹ Universidad Autónoma de Baja California. Instituto de Investigaciones Oceanológicas, Carretera Ensenada-Tijuana No. 3917, Frac. Playitas, Ensenada, Baja California, CP 22810, México.

² Universidad Autónoma de Baja California, Facultad de Ciencias Marinas, Carretera Tijuana-Ensenada No. 3917, CP 22860, Frac. Playitas, Ensenada, Baja California, 22860, México, México.

³ Departamento de Oceanografía Biológica, CICESE. Carretera Ensenada-Tijuana No. 3918, Frac. Playitas, C.P. 22860, Ensenada, Baja California, México

* Corresponding author. E-mail: fdelgadillo@uabc.edu.mx, Phone: +52-646-174-4601 x154.

Key Points:

- A significant reduction of nitrate concentrations and total chlorophyll-*a* was attributed to the marine heatwave in 2014 and El Niño in 2015
- Size fractionated Chl-*a* showed that smaller cells predominated over larger cells, contributing with the higher proportion of total Chl-*a*
- A shift towards an oligotrophic state occurred in nearshore surface waters off northern Baja California during the warm period of 2014-2015

42

43

44 **Abstract**

45 We report the seasonal variability of temperature, nutrients, and total and size fractionated
46 chlorophyll-*a* in nearshore waters off northern Baja California (nBC), under conditions of
47 the marine heatwave and El Niño that occurred in the northeastern Pacific during
48 2014-2015. Compared with 2008-2012, our study period was characterized by warmer
49 waters, nitrate-impooverished and with very low chlorophyll-*a* concentration, which was
50 closely associated with strong stratification and reduced upwelling conditions off nBC.
51 Temperature anomalies were $>3.0^{\circ}\text{C}$ by the end of 2014 when the marine heatwave
52 prevailed, decreased during the spring-early summer upwelling season of 2015, and
53 returned to $>3.5^{\circ}\text{C}$ by the end of 2015 when El Niño appeared along the coast of nBC. As
54 in 2008-2012 and closely coupled with upwelling, a clear seasonal cycle of total
55 chlorophyll-*a* was recorded under these abnormally warm conditions. However, total
56 chlorophyll-*a* and nitrate concentrations were significantly reduced (25-68% and 33-90%,
57 respectively), with negative anomalies throughout the study period. Moreover, the seasonal
58 evolution of the size-fractionated chlorophyll-*a* concentration showed that smaller cells
59 ($<5\ \mu\text{m}$) systematically contributed with the largest fraction ($>60\%$) of the total
60 chlorophyll-*a*. Our findings indicate that the sequential occurrence of the marine heatwave
61 in 2014 and El Niño in 2015, had a significant and sustained impact limiting the nitrate
62 supply and reducing the total chlorophyll-*a* in nearshore waters off nBC. In conclusion,
63 our data reveal that a shift towards an oligotrophic state occurred in nearshore surface
64 waters off northern Baja California during the warm period of 2014-2015.

65

66 **Keywords:** size-fractionated chlorophyll-*a*, nitrate, 2014 Heatwave, El Niño 2015,
67 California Current System

1. Introduction.

Located in the southern section of the California Current System (CCS), the coastal zone off the Baja California peninsula is an upwelling system that sustains a rich, diverse, and highly productive ecosystem. Such high primary production is largely due to wind-driven coastal upwelling taking place mostly during the spring and early summer seasons (Linacre et al., 2010a). Besides, this region is considered as an oceanographic transition zone, where the cold and low-salinity water of the California Current meets seasonally with warmer and saltier waters of tropical/subtropical origin (Durazo et al., 2010; Durazo, 2015; Kurczyn et al., 2019). Given that most of the biological and hydrographic variability in this region occurs at the seasonal and inter-annual time scales, it is valuable to understand how the system functioning is impacted by any other phenomena that adds or decreases variability at these time scales.

During 2014–2015, unusually warm sea surface temperatures were recorded throughout the CCS (e.g., Bond et al., 2015; Robinson, 2016), which resulted in major disturbances of considerable ecological and economic impacts (Cavole et al., 2016; Brodeur et al., 2019; Lavaniegos et al., 2019). The first anomalously warm condition was initially observed during the winter of 2013–2014, when the waters off the coast of Alaska showed anomalously high temperatures (Gentemann et al., 2017). Then, during 2014, the patch of warm water (hereafter 2014-HW for heatwave) appeared along the coast of Baja California in the southernmost part of the CCS (Avila-Lopez et al., 2016; Di Lorenzo & Mantua, 2016; Durazo et al., 2017; Gómez-Ocampo et al., 2017; 2018; Rudnick et al., 2017). Such thermal anomaly in surface waters of the northeastern Pacific was due to a persistent high-pressure ridge that inhibited winter mixing, preventing typical cooling of surface waters (Bond et al., 2015; Siedlecki et al., 2016), and enhanced northward surface ocean transport by anomalous easterly winds (Freeland & Whitney, 2014; Peterson et al., 2015). In particular, warm anomalies off Southern California were linked to local anomalous atmospheric forcing including weak winds and high downward heat flux, apparently unrelated to the equatorial Pacific (Zaba & Rudnick, 2016). However, it is still unclear if the warm patch in the southernmost extension of the CCS was originated by advection or by local or regional changes in ocean-atmosphere heat fluxes.

By the end of 2015, a strong El Niño developed in the eastern equatorial Pacific and a pulse of warm water moved along the coast in the northeastern Pacific, producing extremely high sea surface temperatures along the coast of the CCS (Di Lorenzo & Mantua,

2016; Jacox et al., 2016; Rudnick et al., 2017). The highest positive temperature anomalies in the Baja California coast were observed in September 2015, followed by a steep decline to neutral conditions in spring 2016 (Durazo et al., 2017; Gómez-Ocampo et al., 2017; Jiménez-Quiroz et al., 2019), raising thus great uncertainty on the potential impacts on the chemical, biological and oceanographic conditions of coastal waters in the southern boundary of the CCS. Here, we describe and discuss the changes that occurred in hydrographic conditions, nutrient concentrations, total chlorophyll-*a* and size-structure of phytoplankton community associated with warmer waters brought to the coastal zone of northern Baja California during the sequential occurrence of the 2014-HW and El Niño over the 2014-2015 period. It is shown that, compared with 2008-2012, increased temperatures, strong stratification and reduced upwelling conditions prevalent in that time, had a significant and sustained impact limiting nitrate supply to the euphotic zone and reducing total chlorophyll-*a*. Lastly, our results show that a shift towards an oligotrophic state took place in nearshore waters off northern Baja California during the warm period of 2014-2015.

2. Study Area

Hydrographic and biological sampling was carried out at Todos Santos Bay (TSB), a semi-enclosed system located on the northwestern coast of Baja California, within the southern section of the CCS (Fig. 1). TSB covers an area of ~180 km², has an average depth of 50 m and communicates with the adjacent Pacific Ocean through two entrances (Argote-Espinoza et al., 1991; Mateos et al., 2009). The northern entrance has a length of 12 km and ~40 m depth, while the southern entrance is ~6 km length and its bottom topography is related with a submarine canyon of ~300 m deep. Off the bay, the continental shelf is very narrow and within the first 5 km towards the open sea, the continental slope descends abruptly (Delgadillo-Hinojosa et al., 2015).

Hydrographic conditions off northern Baja California (nBC) are characterized by the presence of the California Current, a year-round equatorward surface flow of cold and low-salinity water of subarctic origin (Durazo, 2015; Kurczyn et al., 2019), and the California Undercurrent, a subsurface poleward flow (100–400 m deep) along the continental margin

characterized by relatively high salinity (Linacre et al., 2010a; Durazo, 2015; Kurczyn et al., 2019). Subarctic water dominates during winter and spring seasons, while tropical and subtropical influences are commonly observed through late summer and autumn (Lynn & Simpson, 1987; Durazo et al., 2010). Moreover, the region is characterized by persistent alongshore winds blowing from the northwest, with a tendency to be stronger during the spring and summer months (Castro & Martínez, 2010). This condition is responsible for inducing coastal upwelling most of the year, although with more intensity during spring and summer seasons (Zaytsev et al., 2003; Pérez-Brunius et al., 2007). Thus, during this period, upwelling brings cold, salty and nutrient-enriched subsurface waters into the euphotic zone, which eventually boost primary production of the surface layer (Espinosa-Carreón et al., 2001; 2004; Gaxiola-Castro et al., 2010; Linacre et al., 2010a).

3. Methodology

3.1. Experimental design and field sampling

A monthly sampling program was carried out at six stations spatially distributed along an inshore-offshore transect off nBC, which covered both the interior of TSB and the adjacent Pacific Ocean (Fig. 1). The sampling program began in August 2014 and ended in December 2015, covering the sampling transect in 17 occasions. In this work, hydrographic, chemical, and biological observations from four of these six stations sampled during 2014-2015, are compared with a similar dataset already collected along the same transect over the 2008-2012 period (see section 3.3). Field work was carried out from a boat and the entire sampling completed within a 6 h period. At each station, CTD casts were carried out up to a maximum depth of 50 m or near to the bottom at stations inside the bay. In addition, sea surface temperature was recorded with a digital thermometer (precision 0.1 °C) and surface water samples were collected (~0.5 m) for analyses of salinity (250 mL), nutrients (30 mL), total chlorophyll-*a* (1000 mL) and size-fractionated chlorophyll-*a* (1000 mL) using individual plastic bottles. Seawater samples for dissolved iron (dFe) analysis were collected using clean techniques described in detail elsewhere (Delgadillo-Hinojosa et al., 2015). Finally, water samples were immediately stored in coolers with ice after collection and kept cold during its transportation to the laboratory.

3.2. Sample Analysis

In the laboratory, the same day of sampling, water samples for total and size-fractionated chlorophyll-*a* determination were filtered using Whatman GF/F filters (~0.7 μm pore size, 25 mm diameter) and polycarbonate Nuclepore membrane filters (~5 μm pore size, 25 mm diameter), respectively. Filters with pigments were individually wrapped in aluminum foil, labeled, and stored in Petri dishes at -20 °C until analyzed. Photosynthetic pigments were extracted with 90% acetone for 24 hours, kept in a cold dark place (Parsons et al., 1984) and quantified with a Cary-50 UV-visible spectrophotometer. In this work, size fractions of chlorophyll-*a* were divided into two classes: large cells (>5 μm) and small cells (>0.7 μm and <5 μm). Small cells fraction was estimated as the difference of total chlorophyll-*a* (>0.7 μm) and chlorophyll-*a* (>5 μm). One caveat of this approach is that pico-sized components (0.2-2 μm) are not fully included in the small-cells category, especially oxyphototrophic cyanobacteria, such as *Prochlorococcus* and *Synechococcus*. However, pico-eukaryote cells larger than 0.7 μm can also be an important fraction of this size-class (e.g., Veldhuis et al., 2005; Linacre et al., 2015).

Samples for inorganic nutrients were passed through GF/F filters and the filtrates stored in LDPE bottles at -20 °C until chemical analysis. Silicate (H_4SiO_4) and nitrate plus nitrite ($\text{NO}_3 + \text{NO}_2$; hereafter nitrate) concentrations were determined using wet chemical colorimetry (Gordon et al., 1993) with a segmented flow analyzer (Skalar SAN Plus). Detection limits for H_4SiO_4 , nitrate and chlorophyll-*a* were 0.04 μM , 0.022 μM and 0.07 mg m^{-3} , respectively. Salinity was measured with a Guildline Autosol 8400B salinometer, calibrated with the International Association for Physical Sciences of the Ocean (IAPSO) standard seawater. Dissolved Fe concentrations were determined by Graphite Furnace Atomic Absorption Spectrophotometry (Agilent Spectra 880Z) after a preconcentration step in a clean-lab using the APDC/DDDC organic extraction method (Bruland et al., 1985; Segovia-Zavala et al., 2010; Félix-Bermúdez, 2018). The accuracy and precision of the method were estimated by analysis of the Certified Reference Material of Seawater NASS-7 (NRC-CNRC; percentage of recovery $102.0 \pm 8.0\%$).

3.3. Temperature, salinity, nitrate and total chlorophyll-*a* anomalies

Seasonal climatologies of sea surface temperature (SST), salinity, nitrate and total chlorophyll-*a* were built with data collected monthly along the same transect (stations 2, 3, 5, 6; Fig. 1) during the period of 2008-2012. An average year (hereafter referred as “climatology”) of SST, salinity, nitrate and total chlorophyll-*a* was constructed by calculating their monthly averages for the inner (stations 2, 3) and outer (stations 5, 6) bay

over the 2008-2012 period (Fig. 1). In the particular case of nitrate, the average year for outer bay also included surface data collected over the 2008-2012 period at Antares station, as well as surface data (for stations near or at the position of our stations 5 and 6), from eight cruises carried out in 2008 (summer and fall), 2009 (winter and spring) and 2011 (winter, spring, summer and fall) in the TSB region (labeled as TSB cruises in Fig. 1). Similarly, the average year for inner bay also considered nitrate surface data from the same cruises, although for stations near or at stations 2 and 3 of our study period. Lastly, time series of monthly anomalies (August 2014 to December 2015) for the inner and outer regions of the bay, were computed by contrasting measured values to the climatological mean.

3.4. Upwelling intensity: climatology and anomalies

The daily Coastal Upwelling Index (CUI) time series (January 2008–December 2016) was obtained from the Pacific Fisheries Environmental Laboratory (PFEL) website (<http://www.pfeg.noaa.gov>). Since our study area is located at approximately 31.8 °N, the daily CUI values of stations at 30.0 and 33.0 °N were averaged for the whole period. Previously, all daily CUI values of each PFEL station exceeding 2.5 standard deviations from the annual mean were eliminated (<1% of the total of each time series) and replaced by the mean of the contiguous values. Next, the climatology of CUI was obtained considering the monthly average for the 2008-2012 period. Finally, monthly CUI anomalies over the 2014-2015 period were calculated by subtracting the monthly climatological value from the monthly CUI for each sampling month.

3.5. Climatology and anomalies of the Biologically Effective Upwelling Transport Index (BEUTI)

BEUTI is an estimate of nitrate flux ($\text{mmol m}^{-1} \text{s}^{-1}$) into the surface mixed layer and provide an index that better captures bottom-up drivers of productivity in the CCS (Jacox et al., 2018), and it is calculated as the product of the estimated vertical transport and nitrate concentration at the base of the mixed layer (Jacox et al., 2015a). The BEUTI time series (January 2008–December 2016) for our study region was obtained from the website <http://mjacox.com/upwelling-indices/>. The climatology of BEUTI was estimated considering the monthly average for our reference period (2008-2012). Then, monthly BEUTI anomalies over the 2014-2015 period were calculated by subtracting the monthly climatological value from the monthly BEUTI for each sampling month.

3.6. Stratification parameter (ϕ) anomalies

The stratification parameter (ϕ ; J m^{-3} ; Simpson, 1981) was used as a measure of the amount of energy required to vertically homogenize the water column; the higher the ϕ , the more stratified the water column. $\phi_{100\text{m}}$ was calculated using 204 CTD profiles recorded outside the bay over the 2008-2016 period. The CTD dataset considered 23 campaigns at station 100.30 of IMECOCAL cruises (Durazo, 2015), as well as all hydrographic stations, located within a radius of 5 km around stations E5-E6, which were carried out during the course of 17 oceanographic cruises (Kurczyn et al., 2019; Delgadillo-Hinojosa unpublished; TSB cruises in Fig. 1). Since our CTD casts outside the bay were performed up to 50 m depth during the 2014-2015 period, $\phi_{100\text{m}}$ for the warm period was estimated with the following linear equation ($\phi_{100\text{m}} = 1.41 * \phi_{50\text{m}} + 52.6$; $r=0.76$, $p<0.001$). Finally, $\phi_{100\text{m}}$ anomalies were calculated for the 2014-2015 period, taking as reference the climatology of $\phi_{100\text{m}}$ for the 2008-2012 period.

3.7. Net primary production (NPP) and Export Flux anomalies

Satellite-based NPP time series (January 2008–December 2016) were retrieved from the Oregon State University website (<https://www.science.oregonstate.edu/ocean.productivity/>) and processed using the SeaDAS 7.3.2 software (<https://seadas.gsfc.nasa.gov/>). In this site, NPP ($\text{g m}^{-2} \text{d}^{-1}$) estimates using the Carbon-based Production Model (CbPM) are available as 8-day composites at a resolution of 9 km. This model combines phytoplankton carbon calculated from the particulate backscattering coefficient, the phytoplankton growth (μ) based on Chl-*a*:C ratios, and light change through the water column (Behrenfeld et al., 2005; Westberry et al., 2008). Time series of monthly NPP for four stations (total area of $14 \times 14 \text{ km}^2$) located immediately off TSB was generated averaging the 8-day composites data over the 2008-2016 period. In this case, stations (S) were positioned at 31.833°N , 116.917°W (S-1); 31.833°N , 116.833°W (S-2); 31.75°N , 116.917°W (S-3); and 31.750°N , 116.833°W (S-4). Lastly, monthly NPP anomalies for the 2014-2015 period were calculated as differences between the monthly NPP time series and the climatology of NPP built for the 2008-2012 period. As an estimate of the biological pump efficiency, Export Flux anomalies for the 2014-2015 period were calculated from NPP for the same period, following the approach of Kahru et al. (2019). This methodology utilizes a quantitative relationship

between net primary production and Export Flux ($EF = 0.08 \times NPP + 72$; EF in $\text{mg C m}^{-2} \text{ d}^{-1}$) recently reported for the southern California Current system (Kahru et al., 2019; Kelly et al., 2018; Morrow et al., 2018).

3.8. The Oceanic El Niño (ONI) and Multivariate El Niño–Southern Oscillation (MEI) indices

As an indication of the existence and strength of El Niño (or La Niña) conditions in our study region, we used both the ONI and MEI time series (January 2008–December 2016), which were obtained from the NOAA website. The ONI index is derived as the 3-month running mean of SST anomalies in the El Niño 3.4 region located at 5°N – 5°S , 170° – 120°W (http://www.cpc.noaa.gov/products/analysis_monitoring/ensostuff/ensoyears.shtml); whereas the MEI index is based on six variables recorded over the tropical Pacific Ocean: sea level pressure, zonal and meridional components of the surface winds, SST, surface air temperature, and total cloudiness fraction of the sky (Wolter & Timlin, 2011; <https://www.esrl.noaa.gov/psd/enso/mei/table.html>)

4. Results

Our analysis of the 17-month record of SST and CTD-temperatures in TSB indicates that there were three distinct oceanographic conditions that occurred sequentially during the study period: (1) the 2014-HW from August 2014 to February 2015, (2) the upwelling season from April to July 2015, and (3) El Niño from August to December 2015 (Fig. 2a–d; Table I). The main hydrographic, chemical and biological changes observed during each of these episodes in 2014–2015, were identified by comparison with the 5-year monthly time series of SST, salinity, nitrate, and total chlorophyll-*a* recorded in the same transect over 2008 to 2012 (see section 3.3).

4.1. Hydrography during the 2014–2015 period

During the 2014–2015 period, SST showed a marked seasonal pattern throughout the study area, with low temperatures in the mid-winter and spring (16 – 17°C) and high in the late summer (21 – 24°C ; Fig. 2a, b). However, when compared with the 2008–2012 climatological cycle, surface waters inside and outside the bay were warmer in 2014–2015 (Fig. 2a, b), with the exception of the samplings of June and July 2015. Outside the bay for instance, mean SST ($20.1 \pm 0.6^{\circ}\text{C}$) recorded during the 2014-HW was similar to that recorded under El Niño ($20.6 \pm 0.4^{\circ}\text{C}$). But both were significantly distinct

(t_{student} , $p < 0.05$) from that recorded during the upwelling season (16.4 ± 0.3 °C), which is evidence of the impact on SST associated with the vertical transport of cold waters from mid-spring to mid-summer 2015 (Fig. 2a, c; Table I). A similar behavior was observed in SST at the inner stations, although surface waters were slightly warmer inside of the bay (Fig. 2b, d; Table I), revealing the retentive nature of this semi-enclosed coastal system.

4.2. Nutrient concentrations

In general, dFe concentrations were temporally variable throughout the study (Table I); however, average dFe concentration inside (4.96 ± 0.35 nM) was significantly higher (t_{student} , $p < 0.05$) than outside the bay (3.60 ± 0.34 nM). In the case of inorganic nutrients, H_4SiO_4 concentrations were very low but there was not differences between the inner (3.71 ± 0.40 μM) and outer bay (3.77 ± 0.28 μM ; Table I). In contrast, nitrate concentrations were almost depleted throughout the period of study, even during the upwelling season when high nutrient levels would be expected (Fig. 2e, f; Table I). Hence, nitrate overall means of 0.23 ± 0.03 μM and 0.31 ± 0.06 μM were recorded in the outer and inner bay, respectively, suggesting that oligotrophic conditions prevailed in this coastal zone during the entire study period.

4.3. Total chlorophyll-*a* (Chl-*a*) and size-fractionated chlorophyll-*a*

Chl-*a* also presented a clear seasonal behavior inside and outside the bay, with highest mean concentrations during spring (2.21 ± 0.35 mg m^{-3}) associated with upwelling intensification, and lowest means during the 2014-HW (0.56 ± 0.11 mg m^{-3}) and El Niño (0.77 ± 0.09 mg m^{-3}) conditions (Fig. 3a, b; Table I). Mean Chl-*a* values recorded during 2014-2015 were significantly lower (t_{student} , $p < 0.05$) than those measured over the 2008-2012 period. Moreover, the small phytoplankton cells were dominant both inside and outside the bay throughout the study, except during the upwelling season when large phytoplankton cells reached the higher values (Fig. 3c, d; Table I). The clearest example was observed outside the bay, where the mean small/large cell ratio reached 3.4 ± 1.0 and 8.4 ± 1.4 during the 2014-HW and El Niño conditions, respectively; whereas during the upwelling season the mean ratio was 1.7 ± 0.5 (Fig. 3e, f; Table I), revealing that there was an important increase of large phytoplankton cells off TSB, linked to the vertical transport of cold waters to the surface.

5.0. Discussion

Over the entire eastern tropical Pacific, warming events at interannual scales are produced by a poleward-propagating equatorial coastally trapped Kelvin wave and by atmospheric teleconnections between equatorial latitudes and tropical and sub-tropical latitudes (Durazo & Baumgartner, 2002). These processes generate positive sea level anomalies in the coastal area, with a consequent deepening of the thermocline, and a considerable increase of upper layer (0-100 m) temperature (Kessler, 2006; Godínez et al., 2010). Interannual warming events are commonly identified as positive values in the ONI and MEI time series. Thus, positive values of such indices during the study period (Fig. 4a) suggests the presence of warmer waters in the coastal zone of nBC. Moreover, this condition was accompanied with the occurrence of anomalous low wind intensities, which caused reduced coastal upwelling along the Pacific coast of nBC (Fig. 4b; Robinson, 2016; Zaba & Rudnick, 2016). In the following sections, we will discuss how these anomalous climatic and oceanographic conditions affected the hydrography, the nutrient supply, the Chl-*a* concentrations and its size structure off the coast of nBC.

5.1. Impacts of the 2014-HW, upwelling and El Niño on SST anomalies

Data from recent literature shows that over the 2014-2015 period, there was a significant increase of nearshore temperature anomalies along the coast of Washington (Gentemann et al., 2017), Oregon (Peterson et al., 2017), California (Zaba & Rudnick, 2016; Chao et al., 2017; Kahru et al., 2018) and Baja California (Robinson, 2016; Gómez-Ocampo et al., 2017; 2018), associated with the sequential occurrence of the 2014-HW and El Niño in 2015. Our hydrographic analysis for nearshore waters in nBC clearly shows that, after removing the seasonal cycle, SST anomalies were approximately 3.0 °C warmer under the 2014-HW conditions, decreased through the 2015 upwelling season, and finally, reached values >3.5 °C when El Niño was already present in the coastal zone (Fig. 5a, b; Table I). These results are comparable to those previously reported for the southern section of the CCS (e.g., Zaba & Rudnick, 2016; Durazo et al., 2017; Rudnick et al., 2017; Kahru et al., 2018; Jiménez-Quiroz et al., 2019). Zaba & Rudnick (2016) and Gentemann et al. (2017) for example, reported that nearshore SST anomalies associated with the 2014-HW first appeared along Southern California in March 2014, increased by August 2014, and remained positive from September 2014 to May 2015. Similarly, Robinson (2016) indicated that off Baja California there was a period of warming, reduction of wind stress and weakened coastal upwelling from May 2014 to April 2015 associated with the 2014-HW. Then, a second process of warming occurred from September to December 2015,

which was due to El Niño. However, during the 2015 upwelling season, the magnitude of SST anomalies decreased notably because the vertical transport of cold deep water played a major role in cooling the surface waters in the region (Zaba & Rudnick, 2016; Durazo et al., 2017; Gentemann et al., 2017).

Besides the changes in SST, both the 2014-HW and El Niño periods showed saltier than normal conditions (Fig. 5c, d), while fresher waters were observed during the upwelling season. Saltier conditions could be due to one or several processes including an increased surface evaporation given by the occurrence of positive SST anomalies, an eastward advection of unusually saltier water from the central Pacific, and/or a coastal poleward advection of tropical surface waters due to the increase of coastal sea level (Durazo et al., 2017). However, Zaba & Rudnick (2016) reported that along-isopycnal salinity in Southern California Bight showed a fresh anomaly during 2014–2015, which was attributed to an onshore displacement of the relatively fresh offshore waters of the California Current (CC). Similarly, Durazo et al. (2017) found that during 2014–2015, the core of the CC off nBC not only moved onshore but also was distributed at depths between 60–120 m. Thus, the lower than usual salinity observed during the upwelling season of 2015 may be due to slightly fresher water being brought to the surface to compensate the offshore Ekman transport. Consequently, the recent nearshore upwelled water, which in normal conditions is the relatively salty, nutrient-rich California Undercurrent (Linacre et al., 2010a; Kurczyn et al., 2019), was replaced by fresher nutrient-poor CC water.

The fact that surface coastal waters off nBC were significantly warmer in 2014–2015 than the 2008–2012 climatological average, led to a more strongly stratified water column (Fig. 4c), as has been previously documented (Gonzalez-Silvera et al., 2016; Gómez-Ocampo et al., 2017). Moreover, the co-occurrence of increased thermal stratification and weaker than normal upwelling-favorable winds (Fig. 4b; Robinson, 2016) could have had a few consequences. The first one is that stratification strengthening requires a larger amount of energy to raise deep isopycnals toward the surface (Kosro et al., 2006; Cavole et al., 2016). The second one is that a stratified water column acts as a barrier that reduce the vertical flux of cool subsurface water to the upper layer (Roemmich & McGowan, 1995; Bograd & Lynn, 2003; Jacox & Edwards, 2011; Zaba & Rudnick, 2016; Gómez-Ocampo et al., 2018; Lilly et al., 2019) and, in consequence, the nutrient input toward the euphotic zone.

Our data provide evidence that there was a limited supply of nutrients to the surface layer of the coast of nBC over 2014–2015 period (Fig. 2e, f). Surface nitrate concentrations

were almost depleted throughout the study period, with overall means of $0.23 \pm 0.03 \mu\text{M}$ and $0.31 \pm 0.06 \mu\text{M}$ in outer and inner bay, respectively. In fact, nitrate-impoverished waters were also detected during the upwelling season, when it would expect higher nutrient levels (Camacho-Ibar et al., 2007; Garcia-Mendoza et al., 2009). Comparatively with 2008-2012, negative nitrate anomalies were also recorded throughout the warm period of 2014-2015 (Fig. 5e, f). Outside the bay for example, these anomalies represented a decrease in nitrate concentration ranging between ~77% (upwelling season) and 90% (2014-HW – El Niño), indicating that nitrate availability was significantly (t_{student} , $p < 0.05$) impacted by the presence of anomalously warm waters along the coast of nBC (Table I). Negative BEUTI anomalies also suggests that the vertical flux of nitrate was reduced throughout the warm period (Fig. 4d; Jacox et al., 2018). Consistent with our results, Lilly et al. (2019) recorded nitrate concentrations $< 1 \mu\text{M}$ and also reported negative nitrate and Chl-*a* anomalies for the Southern California Bight throughout the durations of the 2014-HW and El Niño in 2015. Overall, this nutrient data analysis implies that associated with ocean warming (Fig. 2a, b; 5a, b) and enhanced stratification (Fig. 4c), there was a reduced vertical transport of nutrients (Figs. 4d; 5e, f; Gonzalez-Silvera et al., 2016; Zaba & Rudnick, 2016; Gómez-Ocampo et al., 2017) toward the euphotic zone during the August 2014 to December 2015 period. Besides, the generalized shortage of nutrients (especially N) provides a strong indication that oligotrophic conditions prevailed in this coastal zone during the entire study period (Fig. 2e, f), which, as shown below, had a profound effect on the size structure and biological activity of phytoplankton.

5.2. Total chlorophyll-*a* anomalies during the 2014 – 2015 period

Our hydrographic analysis provides evidence of the occurrence of positive SST anomalies during most of the 2014-2015 period. Still, a question that arises is how phytoplankton was impacted by these anomalously warm waters that appeared in our study area. As can be seen in Figure 3a, b, the seasonal pattern of Chl-*a* was broadly consistent with the seasonality of Chl-*a* recorded in the same transect over the 2008-2012 period. The highest values were recorded in spring/midsummer, suggesting a close coupling between Chl-*a* concentrations and the nutrient supply associated with upwelling off the bay (Gaxiola-Castro et al., 2008; Delgadillo-Hinojosa et al., 2015; Dorantes-Gilardi & Rivas, 2019). In fact, a significant positive correlation was found between the mean monthly Chl-*a* and the monthly CUI, both for the reference period of 2008-2012 ($r = 0.60$; $p < 0.05$; Fig. 6a) and for the warmer period of 2014-2015 ($r = 0.48$; $p < 0.05$; Fig. 6b), implying that

upwelling can stimulate the growth of phytoplankton in our study region, even when in the latter there were conditions of reduced upwelling (Fig. 4b).

Despite that, Chl-*a* concentrations were clearly diminished throughout the study area during the whole warm period, as indicated by the persistently negative anomalies (Fig. 5g, h). The strongest impact was recorded in the inner bay, where Chl-*a* anomalies reached negative values ($-1.44 \pm 0.27 \text{ mg m}^{-3}$) during the 2014-HW, decreased during the 2015 upwelling season ($-0.79 \pm 0.27 \text{ mg m}^{-3}$), and then became more negative ($-0.99 \pm 0.22 \text{ mg m}^{-3}$) by the second half of 2015 under El Niño conditions (Table I). Comparatively with the Chl-*a* levels recorded during 2008-2012, Chl-*a* anomalies reported here represent a diminution ranging between ~26% (upwelling season) and 35% - 68% (2014-HW – El Niño), indicating that phytoplankton community was significantly affected by the presence of anomalous warmer waters that arrived at the coast of nBC (Table I). These results are consistent and complement previous studies that have reported decreased Chl-*a* content in the coastal and open ocean of Southern California (Gómez-Ocampo et al., 2018; Kahru et al., 2018) and Baja California under the 2014-HW and El Niño conditions (Gonzalez-Silvera et al., 2016; Gómez-Ocampo et al., 2017; Mirabal-Gómez et al., 2017; Ortiz-Ahumada et al., 2018; Jiménez-Quiroz et al., 2019). Our analysis indicates that the reduction of Chl-*a* concentration over the 2014-2015 period was closely linked to the strong stratification promoted by the warm waters during the 2014-HW and El Niño (Figs. 4c, 5g, h; Gonzalez-Silvera et al., 2016; Gómez-Ocampo et al., 2017; 2018), as well as reduced upwelling in spring-summer of 2015 (Fig. 4b; Robinson, 2016; Jiménez-Quiroz et al., 2019), which inhibited the regular upward flux of nutrients to the euphotic zone (Figs. 4d; 5e, f; Jacox & Edwards, 2011; Jacox et al., 2015b; 2018; Gonzalez-Silvera et al., 2016). Furthermore, the Fe:nitrate and Si:nitrate ratios (King & Barbeau, 2011; Biller & Bruland, 2014) indicate that there was a preferential drawdown of inorganic nitrogen relative to iron and silicate (Table I), which had as a consequence a general dearth of this nutrient in our study area. Therefore, a nitrogen limited system was developed that resulted in an ecosystem with low Chl-*a*, reduced net primary production and dominated by small sized phytoplankton, all biological characteristics typical of oligotrophic environments (Figs. 2e, f; 3a-f; 4e).

5.3. Shifts in phytoplankton community structure over the 2014-2015 period

The classic herbivorous food-web in active coastal upwelling systems is described as dominated by large primary phytoplankton, such as diatoms and dinoflagellates, which are

grazed by suspension-feeding zooplankton (e.g., copepods and euphausiids), which in turn provides the fuel required to sustain higher trophic levels (e.g., Kudela et al., 2008). However, this conceptual model is not necessarily universal and entirely valid for the nBC upwelling regime, especially when upwelling is null or weak, and/or when heat waves or El Niño events as those described here, occur. In addition to reduced Chl-*a* concentrations, our size fractionated Chl-*a* data shows that the phytoplankton community was consistently dominated by small cells (Fig. 3c-f). As evidence, data in Table I shows that mean small/large cell ratios ranging between 2.7 to 8.4 were recorded during the 2014-HW and El Niño conditions. The exception occurred during the upwelling season of 2015, when there was a significant increase (t_{student} , $p < 0.05$) in chlorophyll-*a* concentrations associated with larger cells and mean small/large cell ratios decreased to ~1.5 (Fig. 3c-f; Table I). Although the seasonal variability of the size-fractionated Chl-*a* in nBC coastal waters has been scarcely investigated, the general pattern reported suggests that phytoplankton biomass is generally dominated by smaller cells along the year (Linacre et al., 2010b). Yet, higher contributions of large sized cells are usually observed during the upwelling season (Gonzalez-Morales et al, 1991; Linacre et al., 2010b; 2012; Martinez-Almeida et al., 2014), suggesting a shift in phytoplankton community structure, seasonally modulated by upwelling events.

In agreement with our findings, a recent study conducted over the 2007-2015 period at a station located 3.8 km offshore from our station 6, reported a marked interannual variability of pigment concentrations, size-structure and community composition of phytoplankton (Gonzalez-Silvera et al., 2016). Based on pigments composition, these authors identified three periods: (1) 2007-2009, characterized by a phytoplankton community dominated by diatoms and dinoflagellates; (2) 2010-to-July-2012, when a notable increase of prymnesiophytes and chrysophytes was observed, and (3) July-2012-to-2015, a period distinguished by the presence of smaller autotrophic groups, very low NO₃ concentrations and a deep euphotic zone associated with the 2014-HW and El Niño 2015 events. In particular, the latter period was characterized by an increase of *Prochlorococcus*, a distinctive cyanobacteria thriving in oligotrophic and highly stratified waters (Hirata et al., 2011; Lewandowska et al., 2014; Gonzalez-Silvera et al., 2016). Similarly, Linacre et al. (2017) studied the temporal variability of picoplankton carbon-biomass at a station located 5 km southeast of our station 6, during March and October 2015. They recorded an increase in carbon-biomass of the cyanobacterial populations, *Prochlorococcus* and *Synechococcus*, linked with the appearance of unusually warm

water in nBC in 2015. Taken together, all these findings provide strong evidence that a shift towards an oligotrophic environment took place in these coastal waters during the warm period of 2014-2015, when the ecosystem clearly presented a general shortage of nitrates, very low Chl-*a* and a predominance of small cells (e.g. [Hirata et al., 2011](#)).

Although our experimental design has its limitations and a detailed response is beyond the scope of this paper; a question that remains open is what factors played a major role regulating the size structure of phytoplankton during the presence of these anomalously warm waters in nearshore nBC. In other words, was there a top-down or bottom-up control on the phytoplankton size structure in that period? Underlying factors invoked in modulating size structure in marine environments, include temperature ([López-Urrutia & Morán, 2015](#)), sinking and grazing ([Acevedo-Trejos et al., 2015](#); [Linacre et al., 2012; 2017](#)) and changes in nutrient supply ([Marañón et al., 2012; 2014](#); [Finkel et al., 2010](#); and references therein). In the case of temperature, this variable influences the metabolic rates of phytoplankton (e.g., [Lewandowska et al., 2014](#); [Sherman et al., 2016](#)); however, we did not find a good relationship between temperature and the small/large cell ratios ($r = 0.11$, $p > 0.05$) in this study. This result suggests that temperature effect was more indirect, since water warming promoted an enhanced stratification and consequent alteration of nutrient supply to the surface waters during these episodes of abnormally warm water in our study area.

On the other hand, zooplankton grazing ‘pushes’ the phytoplankton community towards larger cell sizes ([Acevedo-Trejos et al., 2013; 2015](#)), and the clear dominance of smaller size cells throughout the study (Fig. 3c-f) might suggest that zooplankton grazing was not a factor controlling size structure of phytoplankton during the 2014-HW and El Niño events ([Lavaniegos et al., 2019](#)). However, in an experiment carried out in October 2015 (i.e. El Niño), [Linacre et al. \(2017\)](#) reported that microzooplankton exerted a strong grazing pressure on phytoplankton biomass ($>70\%$ [Chl-*a*]) and daily primary production ($>100\%$ PP). Thus, their data suggest that the low Chl-*a* recorded during El Niño 2015 could also be explained by microzooplankton grazing and thereby, this process cannot be completely ruled out. In contrast, these authors also indicated that in April 2016 there was a return to typical spring conditions with a reduced impact of microzooplankton on all phytoplankton components (protistan consumption of about one third of PP) and a predominance of diatoms ([Linacre et al., 2017](#)). Similarly, during the upwelling season of 2015, we found that both phytoplankton sizes augmented simultaneously (Fig. 3c, d), suggesting that both smaller and larger cells were stimulated by nutrient supply responding

to favorable conditions for growth, what should overcome zooplankton grazing during that season (Lavaniegos et al., 2019).

In the case of nutrient supply, there are several lines of evidence indicating that there was a bottom-up control on phytoplankton size during the occurrence of anomalously warm waters along the coast of nBC. First, there was a general shortage of nutrients (Fig. 2e, f) and below normal net primary production (Fig. 4e) associated with ocean warming and strengthened stratification (Figs. 2, 4c), indicating that there was a limited nutrient supply toward the euphotic zone (particularly nitrate, Fig. 4d; Jacox & Edwards, 2011; Gonzalez-Silvera et al., 2016; Zaba & Rudnick, 2016; Gómez-Ocampo et al., 2017; Lilly et al., 2019). Nitrate depletion and stratified conditions may have benefited smaller phytoplankton, since small cells have higher surface area/volume ratios, which provides them with the ability to compete for nutrients in oligotrophic environments (Chisholm, 1992; Marañón et al., 2012; 2014; Sommer et al., 2017). Second, the percentage of chlorophyll-*a* contained in cells <5 µm was correlated with CUI ($r = -0.57$, $p < 0.05$), suggesting that there was a clear dependence between the variability of phytoplankton cell size and upwelling intensity (Fig. 6c). Smaller cells predominated when upwelling conditions were weak and oligotrophic conditions were stronger. In contrast, smaller cells decreased while large cells increased under active upwelling conditions and oligotrophy was temporally relieved. These results are consistent with previous works indicating that smaller cells thrive in oligotrophic environments and large cells in eutrophic systems (Hirata et al., 2011; Ward et al., 2012; Acevedo-Trejos et al., 2015; López-Urrutia & Morán, 2015), and clearly point out the occurrence of an oligotrophication event in nBC during the sequential occurrence of the 2014-HW and El Niño in 2015.

5.4. Biogeochemical implications of oligotrophication over the 2014-2015 period

Conditions of diminished phytoplankton availability can cause a wide variety of impacts on higher trophic levels (Cavole et al., 2016) whereas decrease in the size of phytoplankton will alter food web structure and the cycling of carbon (Marañón et al., 2003; Finkel et al., 2010; Sommer et al., 2017). The warm anomalies that occurred over the 2014-2015 period in the upper layer of the water column of nBC, negatively impacted the epipelagic ecosystem of the southern CCS, reducing dramatically the phytoplankton available for upper trophic levels and possibly the flux of organic matter to deep waters. During that period, a condition of oligotrophy was developed where small phytoplankton cells predominated. These changes in the phytoplankton size structure probably led to

ecological and biogeochemical shifts in this upwelling system, owing to small cells have slower sinking rates (Finkel et al., 2010; Acevedo-Trejos et al., 2015) and smaller grazers could be potentially favored by an increased presence of small phytoplankton cells (Linacre et al., 2010b; 2012; 2017). Thus, a smaller share of primary production likely was channeled to the classic phytoplankton, crustacean zooplankton, fish food chain, leading to decreased ecological efficiency (Gonzalez-Silvera et al., 2016; Gómez-Ocampo et al., 2017; 2018; Sommer et al., 2017). Furthermore, a higher proportion of primary production likely was respired within the microbial food web favoring the recycling of organic matter in the upper water column, and consequently, the biological pump could have been less efficient in transporting particulate organic matter to deeper waters of the coastal zone of nBC.

To explore this idea, Export Flux (and their anomalies) for our study period in nBC can be estimated from NPP using the equation reported for the CCS (Kahru et al., 2019; Kelly et al., 2018; Morrow et al., 2018). These calculations indicate that, compared with the 2008-2012 period, Export Flux anomalies were below normal with values ranging between $-29.7 \text{ mg C m}^{-2} \text{ d}^{-1}$ during the 2014-HW and $-15.9 \text{ mg C m}^{-2} \text{ d}^{-1}$ during El Niño in 2015 (Table I), suggesting that the biological pump in coastal waters off nBC was less efficient during the warm period. However, a recent quasi-Lagrangian study off Southern California reported measurements of carbon export from the euphotic zone during the 2014-HW, at the end of El Niño 2016, and El Niño-neutral years (Morrow et al., 2018). No substantial differences were found in the relationships between vertical carbon export and its presumed drivers (primary production, mesozooplankton grazing) between warm and neutral years. The framework they used provide measurements of vertical carbon export in timescales of 2-5 days (Morrow et al., 2018); thereby, their results are a snapshot of the ecosystem state (Kelly et al., 2018) and not an estimate of the total vertical carbon export, for instance, at the end of the entire event of the 2014-HW. Consequently, the hypothesis that the biological pump was less efficient during the 2014-HW and/or El Niño 2015 require more data and remains to be proven.

6. Conclusions

The hydrographic dataset presented here shows that, when compared with the reference period of 2008-2012, anomalous hydrographic conditions off the coast of nBC persisted during 2014-2015. External and local factors played an important role in determining the occurrence of these circumstances. The external forcing was the arrival of

warmer waters brought by the 2014-HW, and the advection of equatorial water transported by El Niño in late 2015. The local one was the occurrence of reduced upwelling conditions along the Pacific coast of the Baja California peninsula during the spring-summer of 2015. Overall, it is shown that these abnormally warm conditions significantly impacted the nitrate concentrations and the total chlorophyll-*a* levels of this coastal region. Our data provide evidence of oligotrophication associated with a reduced upward flux of nutrients into the euphotic zone due to a strengthening of stratification in the coastal zone of nBC. A clear seasonal cycle of total Chl-*a* was recorded; however, Chl-*a* concentrations were significantly reduced (25% - 68%) compared with the reference period. Hence, persistently negative anomalies of Chl-*a* were strongly linked with below normal net primary production and with nitrate impoverished waters (33% - 90%) throughout the study. Moreover, size fractionated Chl-*a* data showed that smaller cells predominated over large cells and systematically contributed with the largest proportion (>60%) of the total Chl-*a*. Lastly, our results show that a shift towards an oligotrophic environment took place in nearshore waters off northern Baja California during the warm period of 2014-2015. Finally, the observed changes in Chl-*a*, size structure and primary production in nBC during the 2014-HW and el Niño in 2015 are not exclusive of the southern CCS; since it could be expected that in other upwelling ecosystems that experience similar extraordinary warm conditions, could occur a parallel shift of trophic status with significant ecological repercussions (e.g., Leising et al., 2015; Whitney, 2015; Cavole et al., 2016; Peña et al., 2019).

Acknowledgments

This work was partially funded by the Consejo Nacional de Ciencia y Tecnología (CONACyT) projects number CB 2008-01-098471 and CB-255602, and by Universidad Autónoma de Baja California projects number 403/1/C/99/12 and 403/1/C/104/18. We would like to thank Aaron Gutierrez, Arturo Siqueiros, Javier García and Mauricio Reyes for their assistance during sampling at sea. We are indebted to two anonymous reviewers for providing insightful comments and suggestions that allowed us to significantly improve our paper. The dataset that support this article is available from Figshare data repository (<https://doi.org/10.6084/m9.figshare.12412889>).

635 **References**

- 636 Acevedo-Trejos, E., Brandt, G., Merico, A., & Smith, S. L. (2013). Biogeographical patterns of
637 phytoplankton community size structure in the oceans. *Global Ecology and*
638 *Biogeography*, 22(9):1060-1070.
- 639 Acevedo-Trejos, E., Brandt, G., Bruggeman, J., & Merico, A. (2015). Mechanisms shaping size
640 structure and functional diversity of phytoplankton communities in the ocean. *Scientific*
641 *reports*, 5, 8918.
- 642 Argote-Espinoza, M.L., Gavidia-Medina, F.J., & Amador-Buenrostro, A. (1991). Wind-
643 induced circulation in Todos Santos Bay, B.C., Mexico. *Atmósfera* 4, 101–115.
- 644 Ávila-López, M. C., Hernández-Ayón, J. M., Camacho-Ibar, V. F., Félix-Bermúdez, A., Mejía-
645 Trejo, A., Pacheco-Ruiz, I., & Sandoval-Gil, J. M. (2016). Air–Water CO₂ Fluxes and
646 Net Ecosystem Production Changes in a Baja California Coastal Lagoon During the
647 Anomalous North Pacific Warm Condition. *Estuaries and Coasts*, doi:10.1007/s12237-
648 016-0178-x.
- 649 Behrenfeld, M. J., Boss, E., Siegel, D. A. & Shea, D. M. (2005). Carbon-based ocean
650 productivity and phytoplankton physiology from space. *Global Biogeochemical Cycles*,
651 19, GB1006, doi:10.1029/2004GB002299.
- 652 Biller, D. V., & Bruland, K. W. (2014), The central California Current transition zone: A broad
653 region exhibiting evidence for iron limitation, *Progress in Oceanography*, 120: 370-382,
654 doi:10.1016/j.pocean.2013.11.002.
- 655 Bograd, S. J., & Lynn, R. J. (2003) Long-term variability in the Southern California Current
656 System, *Deep Sea Research Part II: Topical Studies in Oceanography*, 50:2355-2370,
657 doi:https://doi.org/10.1016/S0967-0645(03)00131-0.
- 658 Bond, N. A., Cronin, M.F., Freeland, H., & Mantua, N. (2015). Causes and impacts of the 2014
659 warm anomaly in the NE Pacific. *Geophysical Research Letters*, 42, 3414–3420,
660 doi:10.1002/2015GL063306
- 661 Brodeur, R. D., Auth, T. D., & Phillips, A. J. (2019) Major Shifts in Pelagic Micronekton and
662 Macrozooplankton Community Structure in an Upwelling Ecosystem Related to an
663 Unprecedented Marine Heatwave. *Frontiers Marine Sciences*. 6:212. doi:
664 10.3389/fmars.2019.00212
- 665 Bruland, K., Coale, K.H., Mart, I., 1985. Analysis of seawater for dissolved Cd, Cu and Pb: an
666 intercomparison of voltammetric and atomic absorption methods. *Marine Chemistry* 17,
667 285–300.
- 668 Castro R., & Martínez, A. (2010). Variabilidad espacial y temporal del campo de viento frente
669 a la península de Baja California. In: Durazo R. and Gaxiola G. (Eds). *Dinámica del*
670 *Ecosistema Pelágico frente a Baja California, 1997–2007*. Instituto Nacional de Ecología
671 (INE)/Centro de Investigación Científica y de Educación Superior (CICESE), México.
- 672 Cavole, L. M., Demko, A. M., Diner, R. E., Giddings, A., Koester, I., Pagniello, C. M. L.,
673 Paulsen, M. L., Ramirez-Valdes, A., Schwenck, S. M., Yen, N. K., Zill, M. E., Franks, P.
674 J. S., Society, T. O. (2016). Biological impacts of the 2013–2015 warm-water anomaly in
675 the Northeast Pacific. *Oceanography* 29, 14. <http://dx.doi.org/10.5670/oceanog.2016.32>.
- 676 Camacho-Ibar, V. F. Durazo, R. Souza, A. J., Santamaria, E., Mejia, A., Hernandez-Ayón, J.
677 M., Gonzalez, A. (2007) Upwelling intensification enhances nutrient supply to a coastal
678 lagoon in Baja California during spring 2005. In: *Science and management:*
679 *observations/syntheses/solutions, 19th biennial conference of the Estuarine Research*
680 *Federation, Providence, Rhode Island*. Estuarine Research Foundation.

- Chao, Y., Farrara, J. D., Bjorkstedt, E., Chai, F., Chavez, F., Rudnick, D. L., Enright, W., Fisher, J. L., Peterson, W. T., et al. (2017). The origins of the anomalous warming in the California coastal ocean and San Francisco Bay during 2014–2016, *Journal of Geophysical Research*, 122, doi:10.1002/2017JC013120.
- Chisholm, S. W. (1992). Phytoplankton size, in *Primary Productivity and Biogeochemical Cycles in the Sea*, edited by P. G. Falkowski and A. D. Woodhead, pp. 213–237, Plenum, New York.
- Delgadillo-Hinojosa, F., Camacho-Ibar, V., Huerta-Díaz, M. A., Torres-Delgado, V., Pérez-Brunius, P., et al. (2015). Seasonal behavior of dissolved cadmium and Cd/PO₄ ratio in Todos Santos Bay: A retention site of upwelled waters in the Baja California peninsula, Mexico. *Marine Chemistry*, 168, 37–48.
- Di Lorenzo E. & Mantua N. (2016). Multi-year persistence of the 2014/15 North Pacific marine heatwave. *Nature Climate Change*, doi: 10.1038/nclimate3082.
- Dorantes-Gilardi, M., & Rivas, D. (2019). Effects of the 2013–2016 Northeast Pacific warm anomaly on physical and biogeochemical variables off northwestern Baja California, derived from a numerical NPZD ocean model. *Deep Sea Research Part II: Topical Studies in Oceanography*, 169, 104668.
- Durazo, R., & T. R. Baumgartner (2002). Evolution of oceanographic conditions off Baja California: 1997–1999. *Progress in Oceanography*. 54, 7–31. doi:10.1016/S0079-6611(02)00041-1.
- Durazo R, Ramírez-Manguilar, A. M., Miranda, L. E., & Soto-Mardones, L. A. (2010). Climatología de variables hidrográficas. En *Dinámica del Ecosistema Pelágico frente a Baja California, 1997–2007*. Gaxiola-Castro, G. & Durazo, R. (Eds), *Dinámica del ecosistema pelágico frente a Baja California: 1997–2007*. Ensenada, México: SEMARNAT, INE, CICESE, UABC:25–57.
- Durazo, R., (2015). Seasonality of the transitional region of the California Current System off Baja California. *Journal of Geophysical Research. Oceans*. 120, 1173–1196. <http://dx.doi.org/10.1002/2014JC010405>.
- Durazo R, Castro, R., Miranda, L. E., Delgadillo-Hinojosa, F., & Mejía-Trejo, A. (2017). Anomalous hydrographic conditions off the northwestern coast of the Baja California Peninsula during 2013–2016. *Ciencias Marinas*: 43(2): 81–92
- Espinosa-Carreón, T.L., Gaxiola-Castro, G., Robles-Pacheco, J.M., & Nájera-Martínez, S. (2001). Temperatura, Salinidad, nutrientes y clorofila a en aguas costeras de la Ensenada Sur de California. *Ciencias Marinas*. 27:397–422.
- Espinosa-Carreón T. L., Strub P. T., Beier E., Ocampo-Torres F., & Gaxiola-Castro, G. (2004). Seasonal and interannual variability of satellite-derived chlorophyll pigment, surface height, and temperature off Baja California. *Journal of Geophysical Research*. 109, C03039, doi:10.1029/2003JC002105.
- Félix-Bermúdez, A., (2018). Balance de masas de hierro disuelto y su interacción biológica en la Bahía de Todos Santos: un sistema con características retentivas influenciado por la Corriente de California y surgencias costeras. PhD Thesis Universidad Autónoma de Baja California.
- Finkel, Z. V., Beardall, J., Flynn, K. J., Quigg, A., Rees, T. A. V., & Raven, J. A. (2010). Phytoplankton in a changing world: cell size and elemental stoichiometry, *Journal of Plankton Research*, 32, 119–137, doi:10.1093/plankt/fbp098.
- Freeland, H. & Whitney. F. (2014). Unusual warming in the Gulf of Alaska. PICES Press, 22(2):51–52.

- 728 García-Mendoza E., Rivas, D., Olivos-Ortiz, A., Almazán-Becerril, A., Castañeda-Vega, C.,
729 Peña-Manjarrez, J. L. (2009). A toxic Pseudo-nitzschia bloom in Todos Santos Bay,
730 northwestern Baja California, Mexico. *Harmful Algae*. 8:493-503.
- 731 Gaxiola-Castro, G., Durazo, R., Lavaniegos, B., De-La-Cruz-Orozco, M. E., Millán-Núñez, E.,
732 Soto-Mardones, L., Cepeda-Morales, J. (2008). Pelagic ecosystem response to interannual
733 variability off Baja California. *Ciencias Marinas* 34: 263 -270.
- 734 Gaxiola-Castro, G. Cepeda-Morales, J., Nájera-Mártinez, S., Espinosa-Carreón, T. L., De la
735 Cruz-Orozco, M. E., Sosa-Avalos, R., et al. (2010). Biomasa y producción del
736 fitoplancton. In: G. Gaxiola-Castro and R. Durazo (Eds), *Dinámica del ecosistema
737 pelágico frente a Baja California: 1997-2007*. Ensenada, México: SEMARNAT, INE,
738 CICESE, UABC.:59-86
- 739 Gentemann, C. L., Fewings, M. R., & García-Reyes, M. (2017). Satellite sea surface
740 temperatures along the West Coast of the United States during the 2014–2016 northeast
741 Pacific marine heat wave, *Geophysical Research Letters*, 44, 312–319,
742 doi:10.1002/2016GL071039.
- 743 Godínez, V. M., E. Beier, M. F. Lavín, and J. A. Kurczyn (2010). Circulation at the entrance of
744 the Gulf of California from satellite altimeter and hydrographic observations. *Journal of
745 Geophysical Research: Oceans*. 115, doi:10.1029/2009jc005705.
- 746 Gómez-Ocampo, E., Durazo, R., Gaxiola-Castro, G., De la Cruz-Orozco, M., & Sosa-Avalos,
747 R. (2017). Effects of the interannual variability of water column stratification on
748 phytoplankton production and biomass at the north zone off Baja California. *Ciencias
749 Marinas*. 43(2):109-122. <http://dx.doi.org/10.7773/cm.v43i2.2759>
- 750 Gómez-Ocampo, E., Gaxiola-Castro, G., Durazo, R., & Beier, E. (2018). Effects of the 2013-
751 2016 warm anomalies on the California Current phytoplankton. *Deep-Sea Research II*.
752 151:64–76. <http://dx.doi.org/10.1016/j.dsr2.2017.01.005>
- 753 González-Morales, A. T. & Gaxiola-Castro, G. (1991). Daily variation of physico-chemical
754 characteristics, biomass and phytoplankton primary production in an upwelling coastal
755 zone of Baja California. *Ciencias Marinas*, 17(3):21-37.
- 756 Gonzalez-Silvera, A., Santamaría-del-Ángel, E., Millán-Núñez, R., Camacho-Ibar, V.,
757 Mercado, A., & Gracia-Escobar, M. F. (2016) The effect of interannual processes on
758 phytoplankton pigments off Northern Baja California Peninsula (Mexico): 2007-2015.
759 *Ocean Optics Conference XXIII*: 1-14
- 760 Gordon, L. I., Jennings Jr., J. C., Ross, A. A., & Krest, J. M. (1993). A suggested protocol for
761 continuous flow automated analysis of seawater nutrients (phosphate, nitrate, nitrite and
762 silicic acid) in the WOCE Hydrographic Program and the Joint Global Ocean Fluxes
763 Study. WOCE Hydrographic Program Office, Methods Manual WHPO 91-1:55 pp.
- 764 Hirata, T., Hardman-Mountford, N. J., Brewin, R. J. W., Aiken, J., Barlow, R., Suzuki, K., et al.
765 (2011). Synoptic relationships between surface Chlorophyll-a and diagnostic pigments
766 specific to phytoplankton functional types. *Biogeosciences*, 8(2), 311-327.
- 767 Jacox, M. G., & Edwards, C. A. (2011). Effects of stratification and shelf slope on nutrient
768 supply in coastal upwelling regions. *Journal of Geophysical Research: Oceans*, 116(C3).
- 769 Jacox, M. G., Bograd, S. J., Hazen, E. L., & Fiechter, J. (2015a). Sensitivity of the California
770 Current nutrient supply to wind, heat, and remote ocean forcing. *Geophysical Research
771 Letters*, 42, 5950–5957. <https://doi.org/10.1002/2015GL065147>
- 772 Jacox, M. G., Fiechter, J., Moore, A. M., & Edwards, C. A. (2015b). ENSO and the California
773 Current coastal upwelling response. *Journal of Geophysical Research: Oceans*. 120,
774 doi:10.1002/2014JC010650.

775 Jacox, M. G., Hazen, E. L., Zaba, K. D., Rudnick, D. L., Edwards, C. A., Moore, A. M., &
776 Bograd, S. J. (2016) Impacts of the 2015–2016 El Niño on the California Current System:
777 Early assessment and comparison to past events. *Geophysical Research Letters*, 43,7072–
778 7080. <http://dx.doi.org/10.1002/2016GL069716>.

779 Jacox, M. G., Edwards, C. A., Hazen, E. L., & Bograd, S. J. (2018). Coastal upwelling revisited:
780 Ekman, Bakun, and improved upwelling indices for the US West Coast. *Journal of*
781 *Geophysical Research: Oceans*, 123(10), 7332-7350.

782 Jiménez-Quiroz, M. C., Cervantes-Duarte, R., Funes-Rodríguez, R., Barón-Campis, S. A.,
783 García-Romero, F. J., Hernández-Trujillo, S., et al. (2019). Impact of “The Blob” and “El
784 Niño” in the SW Baja California Peninsula: Plankton and Environmental Variability of
785 Bahía Magdalena. *Frontiers in Marine Science*, 6: doi=10.3389/fmars.2019.00025

786 Kahru, M., Jacox, M. G., & Ohman, M. D. (2018). CCE1: Decrease in the frequency of oceanic
787 fronts and surface chlorophyll concentration in the California Current System during the
788 2014–2016 northeast Pacific warm anomalies. *Deep Sea Research Part I: Oceanographic*
789 *Research Papers*, 140, 4-13.

790 Kahru, M., Goericke, R., Kelly, T. B., & Stukel, M. R. (2019). Satellite estimation of carbon
791 export by sinking particles in the California Current calibrated with sediment trap data.
792 *Deep Sea Research Part II: Topical Studies in Oceanography*, 104639.

793 Kelly, T. B., Goericke, R., Kahru, M., Song, H., & Stukel, M. (2018). CCE II: Spatial and
794 interannual variability in export efficiency and the biological pump in an eastern
795 boundary current upwelling system with substantial lateral advection. *Deep Sea Research*
796 *Part I: Oceanographic Research Papers*, 140, pp. 14-25

797 Kessler, W. S. (2006). The circulation of the eastern tropical Pacific: A review. *Progress in*
798 *Oceanography*. 69, 181-217. doi:10.1016/j.pocean.2006.03.009.

799 King, A. L., & Barbeau, K. A. (2011). Dissolved iron and macronutrient distributions in the
800 southern California Current System, *Journal of Geophysical Research-Oceans*, 116,
801 doi:10.1029/2010jc006324.

802 Kosro, P. M., Peterson, W. T., Hickey, B. M., Shearman, R. K., & Pierce, S. D. (2006). Physical
803 versus biological spring transition: 2005, *Geophysical Research Letters*, 33, L22S03,
804 doi:10.1029/2006GL027072.

805 Kudela, R. M., Banas, N. S., Barth, J. A., Frame, E. R., Jay, D. A., Largier, J. L., et al. (2008),
806 New Insights into the Controls and Mechanisms of Plankton Productivity in Coastal
807 Upwelling Waters of the Northern California Current System. *Oceanography*, 21(4), 46-
808 59.

809 Kurczyn, J. A., Pérez-Brunius, P., López, M., Candela, J., Delgadillo-Hinojosa, F., & García-
810 Mendoza, E. (2019). Water masses and ocean currents over the continental slope off
811 northern Baja California. *Journal of Geophysical Research: Oceans*, 124, 2803
812 – 2823. <https://doi.org/10.1029/2018JC013962>.

813 Lavaniegos, B. E., Jiménez-Herrera, M., & Ambriz-Arreola, I. (2019). Unusually low
814 euphausiid biomass during the warm years of 2014–2016 in the transition zone of the
815 California Current. *Deep Sea Research Part II: Topical Studies in Oceanography*, 169,
816 104638.

817 Leising, A. W., Schroeder, I. D., Bograd, S. J., Abell, J., Durazo, R., Gaxiola-Castro, G., et al.
818 (2015). State of the California Current 2014-15: Impacts of the Warm-Water"
819 Blob". *California Cooperative Oceanic Fisheries Investigations Reports*, 56:1-68

820 Lewandowska, A. M., Boyce, D. G., Hofmann, M., Matthiessen, B., Sommer, U., & Worm, B.
821 (2014). Effects of sea surface warming on marine plankton. *Ecology Letters* 17(5), 614–
822 623.

823 Lilly, L. E., Send, U., Lankhorst, M., Martz, T. R., Feely, R. A., Sutton, A. J., & Ohman, M. D.
824 (2019). Biogeochemical Anomalies at Two Southern California Current System Moorings
825 During the 2014–2016 Warm Anomaly-El Niño Sequence. *Journal of Geophysical*
826 *Research: Oceans*, 124(10), 6886-6903.

827 Linacre, L. Durazo, R., Hernández-Ayón, J. M., Delgadillo-Hinojosa, F., Cervantes-Díaz, G.,
828 Lara Lara, J. R., et al. (2010a). Temporal variability of the physical and chemical water
829 characteristics at a coastal monitoring observatory: Station ENSENADA.
830 *Continental Shelf Research*, 30: 1730-1742.

831 Linacre, L., Landry, M.R., Lara-Lara, J.R., Hernández-Ayón, J., & Bazán-Guzmán, C.A.
832 (2010b). Picoplankton dynamics during contrasting seasonal oceanographic conditions at
833 a coastal upwelling station off Northern Baja California, México. *Journal of Plankton*
834 *Research*, 32(4).

835 Linacre, L., Landry, M. R., Cajal-Medrano, R., Lara-Lara, J. R., Hernández-Ayón, J. M.,
836 Mouriño-Pérez, R. R., Bazán-Guzmán, C. (2012). Temporal dynamics of carbon flow
837 through the microbial plankton community in a coastal upwelling system off northern
838 Baja California, Mexico. *Marine Ecology Progress Series*, 461, 31-46.

839 Linacre, L., Lara-Lara, R., Camacho-Ibar, V., Herguera, J. C., Bazán-Guzmán, C., & Ferreira-
840 Bartrina, V. (2015). Distribution pattern of picoplankton carbon biomass linked to
841 mesoscale dynamics in the southern Gulf of Mexico during winter conditions. *Deep Sea*
842 *Research Part I: Oceanographic Research Papers*. 106:55-67.

843 Linacre, L., Lara-Lara, J. R., Mirabal-Gómez, U., Durazo, R., & Bazán-Guzmán, C. (2017).
844 Microzooplankton grazing impact on the phytoplankton community at a coastal
845 upwelling. *Ciencias Marinas*, 43(2), 93-108.

846 López-Urrutia, Á., & Morán, X. A. G. (2015). Temperature affects the size-structure of
847 phytoplankton communities in the ocean. *Limnology and Oceanography*, 60(3): 733-738.

848 Lynn, R. J., & Simpson, J. J. (1987). The California Current System: The seasonal variability
849 of its physical characteristics. *Journal of Geophysical Research: Oceans*, 92(C12),
850 12947-12966.

851 Martínez-Almeida V. M., Gaxiola-Castro G., Durazo, R., & Lara-Lara, J. R. (2014).
852 Phytoplankton size-fractioned chlorophyll-a off Baja California during winter, spring and
853 summer 2008. *Hidrobiológica*, 24(3):167-181.

854 Marañón, E., Behrenfeld, M. J., González, N., Mouriño, B., & Zubkov, M. V. (2003). High
855 variability of primary production in oligotrophic waters of the Atlantic Ocean: uncoupling
856 from phytoplankton biomass and size structure. *Marine Ecology Progress Series*, 257, 1-
857 11.

858 Marañón, E., Cermeño, P., Latasa, M., & Tadonleke, R. D. (2012). Temperature, resources, and
859 phytoplankton size structure in the ocean. *Limnology & Oceanography*. 57: 1266–1278.
860 doi:10.4319/lo.2012.57.5.1266

861 Marañón, E., Cermeño, P., Huete-Ortega, M., López-Sandoval, D., Mouriño-Carballido, B., &
862 Rodríguez-Ramos, T. (2014). Resource supply overrides temperature as a controlling
863 factor of marine phytoplankton growth. *PLoS One* 9: e99312.
864 doi:10.1371/journal.pone.0099312.

- Mateos E, Marinone SG, & Parés-Sierra A. (2009). Towards the numerical simulation of the summer circulation in Todos Santos Bay, Ensenada, B.C. Mexico. *Ocean Modelling*, 27:107-112.
- Mirabal-Gómez, U., Álvarez-Borrego, S., & Lara-Lara, J. R. (2017). Satellite-derived phytoplankton biomass and production variability in 2 contrasting coastal areas: off southern California and off northern Baja California. *Ciencias Marinas*, 43(4):229-248. doi: 10.7773/cm.v43i4.2763.
- Morrow, R. M., Ohman, M. D., Goericke, R., Kelly, T. B., Stephens, B. M., & Stukel, M. R. (2018). CCE V: Primary production, mesozooplankton grazing, and the biological pump in the California Current Ecosystem: Variability and response to El Niño. *Deep Sea Research Part I: Oceanographic Research Papers*, 140, 52-62.
- Ortiz-Ahumada, J. C., Álvarez Borrego, S., & Gómez Valdés, J. (2018). Effects of seasonal and interannual events on satellite-derived phytoplankton biomass and production in the southernmost part of the California Current System during 2003-2016. *Ciencias Marinas*, 44(1), 1-20. doi: 10.7773/cm.v44i1.2743.
- Parsons, T.R., Maita, Y., & Lalli, C.M. (1984). A Manual of Chemical and Biological Methods for Seawater Analysis. Pergamon Press, New York (173 pp.)
- Peña, M. A., Nemcek, N., & Robert, M. (2019) Phytoplankton responses to the 2014–2016 warming anomaly in the northeast subarctic Pacific Ocean, *Limnology and Oceanography*, 64(2), 515-525, doi:10.1002/lno.11056.
- Pérez-Brunius P, López M., Parés-Sierra A., Pineda, J. (2007). Comparison of upwelling indices off Baja California derived from three different wind data sources. *CalCOFI Reports*, 48:204-214.
- Peterson, W., Robert, M., & Bond, N. (2015). The warm blob-Conditions in the northeastern Pacific Ocean. *PICES Press*, 23(1):36.
- Peterson, W. T., Fisher, J. L., Strub, P. T., Du, X., Risien, C., Peterson, J., & Shaw, C. T. (2017). The pelagic ecosystem in the Northern California Current off Oregon during the 2014–2016 warm anomalies within the context of the past 20 years, *Journal of Geophysical Research: Oceans*, 122, 7267– 7290, doi:10.1002/2017JC012952.
- Robinson, C. J. (2016). Evolution of the 2014–2015 sea surface temperature warming in the central west coast of Baja California, Mexico, recorded by remote sensing, *Geophysical Research Letters*, 43, 7066–7071, doi:10.1002/2016GL069356.
- Roemmich, D., & McGowan, J. (1995). Climatic warming and the decline of zooplankton in the California Current. *Science*, 267, 1324-1326, doi:10.1126/science.267.5202.1324.
- Rudnick, D. L., Zaba, K. D., Todd, R. E., & Davis, R. E. (2017). A climatology of the California Current System from a network of underwater gliders. *Progress in Oceanography*, 154, 64-106.
- Segovia-Zavala, J. A., Lares, M. L., Delgadillo-Hinojosa, F., Tovar-Sánchez, A., & Sañudo-Wilhelmy, S. A. (2010). Dissolved iron distributions in the central region of the Gulf of California, Mexico. *Deep Sea Research Part I: Oceanographic Research Papers*, 57, 53-64.
- Sherman, E., Moore, J. K., Primeau, F., & Tanouye, D. (2016), Temperature influence on phytoplankton community growth rates, *Global Biogeochemical Cycles*, 30(4), 550-559, doi:10.1002/2015GB005272.

- Siedlecki, S., Bjorkstedt, E., Feely, R., Sutton, A., Cross, J., & Newton, J. (2016). Impact of the Blob on the Northeast Pacific Ocean biogeochemistry and ecosystems. *US Clivar Variations*, 14(2):7-12
- Simpson, J. (1981). The shelf-sea fronts: implications of their existence and behavior. *Philosophical Transactions of the Royal Society of London. Series A. Mathematical and Physical Sciences*. 302, 531-546.
- Sommer, U., Peter, K. H., Genitsaris, S., & Moustaka-Gouni, M. (2017). Do marine phytoplankton follow Bergmann's rule sensu lato? *Biological reviews of the Cambridge Philosophical Society*, 92 2, 1011-1026
- Veldhuis, M. J. W., Timmermans, K. R., Croot, P., & van der Wagt, B. (2005) Picophytoplankton; a comparative study of their biochemical composition and photosynthetic properties. *Journal of Sea Research*. 53(1–2):7-24.
- Ward, B. A., Dutkiewicz, S., Jahn, O., & Follows, M. J., (2012), A size-structured food-web model for the global ocean. *Limnology and Oceanography*, 57, doi: 10.4319/lo.2012.57.6.1877.
- Westberry T., Behrenfeld M. J., Siegel D. A., & Boss, E. (2008). Carbon-based primary productivity modeling with vertically resolved photoacclimation. *Global Biogeochemical Cycles*, 22, GB2024.
- Whitney, F. A. (2015) Anomalous winter winds decrease 2014 transition zone productivity in the NE Pacific, *Geophysical Research Letters*, 42(2), 428-431, doi:10.1002/2014gl062634.
- Wolter, K., & Timlin, M. S. (2011). El Niño/Southern Oscillation behaviour since 1871 as diagnosed in an extended multivariate ENSO index (MEI. ext). *International Journal of Climatology*, 31(7), 1074-1087.
- Zaytsev, O., Cervantes-Duarte, R., Montante, O., & Gallegos-Garcia, A. (2003). Coastal upwelling activity on the Pacific shelf of the Baja California Peninsula. *Journal of Oceanography*, 59:489-502
- Zaba, K. D., & Rudnick, D. L. (2016). The 2014–2015 warming anomaly in the Southern California Current System observed by underwater gliders, *Geophysical Research Letters*, 43, doi:10.1002/2015GL067550.

Table Legend

Table I.- Average (\pm standard error) of Hydrographic, Chemical and Biological Variables Measured in Surface Water Collected from the Inner and Outer Bay Under the 2014-HW (Sep-Dec, 2014), Upwelling (Apr-Jul, 2015) and El Niño (Sep-Dec, 2015) Conditions. Mean Monthly Anomalies (Relative to 2008-2012) of Sea Surface Temperature, Salinity, CUI, ϕ_{100m} , Chl-*a*, Nitrate, BEUTI, Satellite-derived Net Primary Production (NPP), and Export Flux for Each Period, Are also Presented

Figure Captions

Figure 1. Map of Todos Santos Bay area in northern Baja California showing the sampling stations. TSB cruises (red star) represents the mean position (within 5 km around stations 5 and 6) for all hydrographic stations sampled during 17 cruises over the 2008-2012 period. The mean annual cycle of nitrate concentration for the outer bay was built using data from stations 5, 6, TSB cruises and Antares. The mean annual cycle of the stratification parameter (ϕ_{100m}) for the outer bay was constructed using CTD data from stations 5, 6, TSB cruises and IMECOCAL 100.30.

Figure 2. Time series of sea surface temperature (SST) for the outer (a) and inner bay (b) over the August 2014 to December 2015 period. Time-depth plot of CTD temperature in (c) the outer bay (average of stations 5 and 6) and (d) inner bay (average of stations 2 and 3) for the same period. The solid lines in panels a and b represent the mean annual cycle of SST (2008–2012) defined as our reference period. Time series of monthly CUI (dotted line) and nitrate surface concentrations (pink circles) for the outer (e) and inner bay (f). The solid lines in panels (e) and (f) show the mean annual cycle of nitrate surface concentration for the 2008–2012 period. We divided our study into three periods: The 2014-HW (from Aug-2014 to Feb-2015); upwelling (from Apr to Jul-2015); and El Niño (from Aug to Dec-2015)

Figure 3. Time series of total chlorophyll-*a* (Chl-*a*), size-fractionated Chl-*a* and small/large phytoplankton cells ratio for surface waters from the outer (a, c, e) and inner bay (b, d, f) over the August 2014 to December 2015 period. The solid lines in panels a and b represent the mean annual cycle (2008–2012) of Chl-*a*. Size-fractionated Chl-*a* was divided into two classes: small cells (<5 μm) and large cells (>5 μm).

Figure 4. Time series of (a) ONI and MEI indices, (b) monthly Coastal Upwelling Index (CUI) anomalies, (c) water column stratification parameter (ϕ_{100m}) anomalies, (d) monthly BEUTI anomalies, and (e) monthly net primary production (NPP) anomalies for the coastal zone of nBC over the 2008 to 2016 period. CUI, ϕ_{100m} , BEUTI and NPP anomalies were calculated relative to the mean annual cycle of each variable for the 2008-2012 period (gray area). Note that from August 2014 to December 2015 (pink area), both ONI and MEI indices, and ϕ_{100m} , remained positive, whereas anomalies corresponding to CUI, BEUTI and NPP, were mostly negative.

Figure 5. Monthly anomalies of sea surface temperature (SST), salinity, nitrate and total chlorophyll-*a* (Chl-*a*) for the outer (a, c, e, g) and inner bay (b, d, f, h) over the period of August 2014 to December 2015. Anomalies for each region were calculated relative to the annual cycle of each variable for the 2008-2012 period.

Figure 6. (a) The relationship between climatologies of the coastal upwelling index (CUI) and total chlorophyll-*a* (Chl-*a*) concentration in Todos Santos Bay for the period of 2008-2012. Relationship between (b) the monthly CUI and Chl-*a*, and (c) the monthly CUI and size-fractionated Chl-*a* in Todos Santos Bay over the 2014-2015 period.